# Thermoelastic effects at low temperatures and quantum limits in displacement measurements

M. Cerdonio* and L. Conti

*INFN Section of Padova and Department of Physics, University of Padova, Italy*

A. Heidmann and M. Pinard

*Laboratoire Kastler Brossel†, 4 place Jussieu, F75252 Paris, France*

(September 29, 2000)

The displacement fluctuations of mirrors in optomechanical devices, induced via thermal expansion by temperature fluctuations due either to thermodynamic fluctuations or to fluctuations in the photon absorption, can be made smaller than quantum fluctuations, at the low temperatures, high reflectivities and high light powers needed to readout displacements at the standard quantum limit. The result is relevant for the design of quantum limited gravitational-wave detectors, both "interferometers" and "bars", and for experiments to study directly mechanical motion in the quantum regime.

**PACS :** 04.80.Nn, 05.40.-a, 42.50.Lc

## I. INTRODUCTION

In a recent paper Braginsky *et al* [1], henceforth BGV, considered the noise in interferometric gravitational-wave detectors due to thermoelastic fluctuations of the mirrors attached to the test masses of the interferometer. These thermoelastic fluctuations have contributions from two independent processes, both acting via the thermal expansivity of the mirror substrate material. The first one is the *thermodynamic* fluctuations in temperature of the body of the mirror substrate (these, in the approximation of small thermal expansion, are independent from the thermodynamic fluctuations in volume, which are responsible for the well studied *thermal* or *brownian* noise [2]). The second one is the *photothermal* temperature fluctuations due to the fact that the number of photons absorbed by the mirror fluctuate.

BGV results for the thermodynamic noise, obtained for half-infinite mirrors, have been extended to the case of finite size mirrors [3], with particular reference to the design of advanced interferometric gravitational-wave detectors, such as LIGOII [4]. In both cases the calculations are concerned with mirrors at room temperature, made of materials well in use for mirrors substrates as fused silica and sapphire, with km long Fabry-Perot cavities, which are characterized by laser beam spots of size $r_0 \simeq 1 \; cm$ and comparatively low finesse $\mathcal{F} \simeq 100$, and with characteristic frequencies $f \simeq 100 \; Hz$, for the mechanical motion to be monitored optically.

There are a number of situations, at variance with the above, which are of interest for optomechanical devices. In such situations one or both of the thermoelastic fluctuations effects may be of concern, when one would like to reach, in the measurements of small displacement, the so called *Standard Quantum Limit* (SQL) [5,6]. Already for LIGOII, BGV seems to discourage, in favour of fused silica, the use of sapphire, which on the other hand may be the material considered for *cold mirrors* in connection with advanced configurations of interferometric gravitational-wave detectors, under study as LCGT [7], LIGOIII [4] and EURO [8].

The BGV effects would be of concern for very sensitive displacement sensors based on high-finesse Fabry-Perot cavities, to be used in connection with bar detectors of gravitational waves as dual cavity transducers [9], or to study the quantum effects of radiation pressure [10–12]. In both cases the cavities are much shorter (less than a few centimeter) than in a gravitational-wave interferometer, the beam spots are smaller ($r_0 \simeq 10^{-2} \; cm$), finesses much larger ($\mathcal{F} \gtrsim 10^5$) and temperatures as low as $T \lesssim 1 \; K$. It may appear from BGV results that the thermoelastic effects would generate particularly large effects, inasmuch the volume involved in the fluctuation processes would be correspondingly smaller.

For these reasons, it is of interest to explore what would be the behaviour of both thermoelastic effects in the low temperatures and small beam spot regimes, where some BGV assumptions break down. In particular, the heat diffusion length $l_t$ depends on the temperature and can become larger than the laser beam spot dimension $r_0$, so that the adiabatic approximation is no longer valid.

In Section II we give the essentials of the regime of phonons and heat propagation, which establishes at low enough temperatures, and we evaluate the thermoelastic noises with a simple calculation, in relation to the beam spot size and to the frequencies at which the optomechanical device is most sensitive.

In Sections III and IV we give an exact calculation of both thermoelastic effects in the whole region of interest,

that is for any value of the ratio $l_t/r_0$. The results, under the assumptions of low temperature regime of Section II, would directly apply to actual mirrors for the quoted optomechanical devices. We also relate in a general way the photothermal noise to the displacement noise induced on the mirror by the quantum fluctuations of radiation pressure in the cavity.

In Section V we discuss limitations and relevance of our approach in the design of the SQL optomechanical displacement devices.

## II. HEAT PROPAGATION AT LOW TEMPERATURES

Let us assume the optomechanical device to work in some frequency range centered around a frequency $f$ and let us discuss the photothermal effect. We revisit the calculation of BGV in the following way, so to use it to see the regime which sets up at low temperatures.

The multilayers coating of the mirror absorbs a small fraction of the light power and this induces an inhomogeneous increase of the temperature of the bulk. The absorbed power is a Poisson distributed random variable (the statistics of the absorbed photon will be discussed in more details in section IV), and these fluctuations lead to thermal fluctuations in the bulk of the mirror. They are consequently responsible for fluctuations of the position of the reflecting face of the mirror, via the thermal expansion of the mirror material.

The r.m.s. displacement noise of the mirror end face $\Delta z = z\alpha\Delta T$ is found by evaluating the r.m.s. fluctuation in temperature $\Delta T$, in a volume $V$ of the mirror of thickness $z$, linear thermal expansion coefficient $\alpha(T)$ and specific thermal capacity $C(T)$, as the absorbed photon flux $n$ fluctuates,

$$\Delta z = z\alpha\frac{\hbar\omega_0\Delta n}{\rho CV}, \qquad (1)$$

where $\hbar\omega_0$ is the energy per photon, $\Delta n = \sqrt{\overline{n}/f}$ is the r.m.s. poissonian fluctuation of the number of photons absorbed over the time $1/f$ ($\overline{n}$ is the average absorbed photon flux), and $\rho$ is the density of the mirror material (axis $z$ is taken normal to the plane face of the mirror).

At room temperature and for large beam spots, BGV conditions apply: the phonon mean free path and relaxation times are very small respectively in comparison to the mirror coating thickness (where the photons create the phonons in the absorption process), and in comparison with the characteristic time $1/f$. The thermal diffusion length at frequency $f$ is given by

$$l_t = \sqrt{\frac{\kappa}{\rho Cf}}, \qquad (2)$$

where $\kappa$ is the thermal conductivity. For a frequency $f$ around $100\ Hz$, $l_t$ is on one hand larger than the coating

thickness $z_c$, and on the other hand much smaller than the beam spot radius $r_0$,

$$z_c < l_t < r_0. \qquad (3)$$

This is the basic BGV approximation, which gives that the volume involved in the fluctuating thermal expansion effect is the fraction of mirror substrate $V \simeq l_t r_0^2$ and thus one has $z \simeq l_t$ in Eq. (1).

This argument reproduces the essential features of BGV spectral density $S_z[f]$ of photothermal displacement noise, as one may write around the frequency $f$,

$$S_z[f] \simeq \frac{\Delta z^2}{f} \simeq \left(\frac{\alpha}{\rho C r_0^2}\right)^2 \frac{S_{abs}}{f^2}, \qquad (4)$$

where $S_{abs} = \hbar\omega_0 W_{abs}$ is the spectral power noise of the absorbed light, with $W_{abs} = \hbar\omega_0\overline{n}$ the average absorbed light power. In fact we see that Eq. (4) is the same final BGV relation (Eq. 8 of [1]), apart from a term with the Poisson ratio of the mirror material and numerical factors.

The condition (3) may break down for small beam spot radius $r_0$ or for low temperature $T$, as the thermal diffusion length gets longer, either in the mirror substrate or in the mirror coating or in both.

For mirrors substrates of crystalline materials, as specifically sapphire, for a frequency $f \simeq 1\ kHz$, the thermal length $l_{ts}$ in the substrate at low temperature gets of the order of 10 $cm$, to be compared with a room temperature value $l_{ts}(300\ K) \simeq 10^{-2}\ cm$ (see Table I). Then at low temperature we rather have

$$l_{ts} \gtrsim r_0, \qquad (5)$$

at all frequencies below some 1 $kHz$, both for mirrors of gravitational-wave interferometers (for which $r_0 \simeq 1.5\ cm$), and for optomechanical sensors (for which $r_0 \leq 3\ 10^{-2}\ cm$). This value for $l_{ts}$ stays constant in the whole region $T \leq 10\ K$, as crystalline materials follow Debye $T^3$ laws for $\alpha(T)$, $C(T)$ and $\kappa(T)$, and thus their ratios are all independent of $T$.

High reflection coatings are typically 40 layers one quarter wavelength thick of alternating amorphous materials as $TiO_2$ and $SiO_2$, with a total thickness $z_c \simeq 10^{-3}\ cm$ for Nd-Yag laser light. For such a coating, the breakdown temperature for Eq. (3) is different for mirrors of large-scale interferometers and for mirrors of high-finesse cavities, because of the difference in $r_0$. For LIGOII mirrors for instance, taking $SiO_2$ as the reference material for the coating, the thermal length $l_{tc}$ in the coating is of the order of $r_0$ only at very low temperature, $T < 1\ K$. Amorphous silica films would have $l_{tc} > 10^{-2}\ cm$ for $T < 10\ K$, so that for high-finesse cavities we have $l_{tc} \gtrsim r_0$ in the whole low temperature region.

Despite this difference, there are two features of relevance, which affect similarly the thermal behaviour of the coating-substrate composite in both types of mirrors.

2

| Fused silica | 300 $K$ | 10 $K$ | 1 $K$ |
|---|---|---|---|
| $\alpha$ $(K^{-1})$ | $5.5\ 10^{-7}$ | $-2.6\ 10^{-7}$ | $-2.6\ 10^{-10}$ |
| $\kappa$ $(W/m.K)$ | 1.4 | 0.1 | $2\ 10^{-2}$ |
| $C$ $(J/Kg.K)$ | $6.7\ 10^2$ | 3 | $3\ 10^{-3}$ |
| $\lambda$ $(m)$ | $8\ 10^{-10}$ | $8\ 10^{-8}$ | $9\ 10^{-6}$ |
| $\alpha/\kappa$ $(m/W)$ | $3.9\ 10^{-7}$ | $2.6\ 10^{-6}$ | $1.3\ 10^{-8}$ |
| $l_t$ $(m)$ | $3\ 10^{-5}$ | $1.2\ 10^{-4}$ | $1.7\ 10^{-3}$ |

| Sapphire | 300 $K$ | 10 $K$ | 1 $K$ |
|---|---|---|---|
| $\alpha$ $(K^{-1})$ | $5\ 10^{-6}$ | $5.8\ 10^{-10}$ | $5.8\ 10^{-13}$ |
| $\kappa$ $(W/m.K)$ | 40 | $4.3\ 10^3$ | 4.3 |
| $C$ $(J/Kg.K)$ | $7.9\ 10^2$ | $8.9\ 10^{-2}$ | $8.9\ 10^{-5}$ |
| $\lambda$ $(m)$ | $5\ 10^{-9}$ | $2.2\ 10^{-3}$ | |
| $\alpha/\kappa$ $(m/W)$ | $1.2\ 10^{-7}$ | $1.4\ 10^{-13}$ | |
| $l_t$ $(m)$ | $1.1\ 10^{-4}$ | 0.11 | |

TABLE I. Thermal properties of fused silica (top) and sapphire (bottom) at different temperatures. The thermal expansion coefficient $\alpha$, thermal conductivity $\kappa$, thermal capacity $C$ and phonon mean free path $\lambda$ are derived from [1] at room temperature, and from [13–15] at low temperatures. The thermal length $l_t$ at 1 $kHz$ is obtained from Eq. (2).

In both cases we have that, at all low temperatures, the thermal length $l_{tc}$ stays longer than the coating thickness, $l_{tc} > z_c$, and that the mean free path $\lambda_s$ of the phonons in the substrate is itself long, at least a fraction of $cm$ [13]. In a coating of a $SiO_2$ film even the phonon mean free path $\lambda_c$ will be larger than $10^{-3}$ $cm$, and thus $\lambda_c > z_c$, for $T \lesssim 1$ $K$ [16].

Let us then consider how the thermal regime changes at sufficiently low temperatures ($T \leq 10$ $K$). The heat delivered by the absorbed photons in the volume $r_0^2 z_c$ of the coating crosses to the substrate in a time smaller than $1/f$, as $l_{tc} > z_c$. From the substrate, as $\lambda_s \gtrsim r_0$, the thermal phonons thereby created will reenter the coating, heating it up in even shorter time over distances $\lambda_s$. This happens because the acoustic mismatch between coating and substrate is small [17], when densities and sound velocities are quite close. The substrate thus acts as a thermal short for the coating in the plane of the mirror end face: the coating and the substrate will be practically isothermal over distances of the order of the phonon mean free path $\lambda_s$ in the substrate. Then the coating will contribute to the thermoelastic fluctuations with its thermal expansion coefficient $\alpha_c$, but following the thermal fluctuations of spectral density $S_T$ of the substrate. On the other hand, at the frequency $f$, the volume of substrate involved in the fluctuating heating will be of the order $V \simeq l_{ts}^3$, where the thermal length is that in the substrate. So, including both the coating and the substrate, we write now for the displacement spectral density $S_z[f]$:

$$S_z[f] \simeq \left( (\alpha_c z_c)^2 + (\alpha_s l_{ts})^2 \right) S_T[f].\tag{6}$$

According to table I, $\alpha_c z_c$ is at least one order of magnitude smaller than $\alpha_s l_{ts}$ at low temperature ($z_c \simeq 10^{-5}$ $m$ and $l_{ts} \simeq 0.1$ $m$). We can then neglect the expansion of the coating over its thickness $z_c$ and we find that the effect is dominated by the substrate properties,

$$S_z[f] \simeq \left( \frac{\alpha_s}{\rho_s C_s l_{ts}^2} \right)^2 \frac{S_{abs}}{f^2}.\tag{7}$$

This is the relevant result of our discussion of thermal behaviour of the coating-substrate composite at low temperature, in that now the temperature fluctuations involve comparatively large substrate volumes, instead of the comparatively small coating volume, where the actual absorption of photons occurs. Notice that, would not this be the case, one would have of course very large effects just concentrated in the volume, the external surface of which is that where displacements are going to be measured at SQL sensitivities.

When we substitute in Eq. (7) the expression (2) for the thermal length, we see a dramatic change of regime,

$$S_z[f] \simeq \left( \frac{\alpha_s}{\kappa_s} \right)^2 S_{abs},\tag{8}$$

where now the (substrate) thermal conductivity $\kappa_s$ appears, instead of the thermal capacity, and the frequency dependence has disappeared. In fact the system behaves as in the low frequency region of a low pass filter, while, under BGV conditions, it was rather in the high frequency region.

We develop in the following sections a rigorous calculation of the effects in the low temperature regime, which gives in clear details the features grossly anticipated above and which can be directly applied to mirrors of interest for optomechanical devices, when the above thermal behaviour of the coating-substrate system is realized.

### III. THERMODYNAMIC NOISE

In this section we determine the thermodynamic noise without any assumption on the ratio $l_t/r_0$ between the thermal diffusion length in the substrate and the beam spot size. Our analysis is an extension of the procedure developed by Liu and Thorne [3], but it is valid even when the adiabatic approximation is not satisfied. According to Eq. (2), the condition $l_t < r_0$ can actually be written as a condition over the frequency, $f > \kappa/\rho C r_0^2$. Our treatment is thus also valid for an angular frequency $\omega = 2\pi f$ smaller than the adiabatic limit $\omega_c$ defined as

$$\omega_c = \frac{\kappa}{\rho C r_0^2}.\tag{9}$$

As shown in the previous section we neglect any effects of the coating, taking only into account the thermal

3

properties of the substrate of the mirror. We also neglect any finite-size effects since we have shown that the volume of substrate involved in the fluctuating heating is usually smaller than the size of the mirror, even at low temperature. We thus approximate the mirror as a half space, the coated plane face corresponding to the plane $z = 0$ in cylindrical coordinates.

The analysis is based on a general formulation of the fluctuation-dissipation theorem, used by Levin [18] to compute the usual thermal noise (brownian motion) of the mirrors in a gravitational-wave interferometer. We know that in an interferometer or in a high finesse Fabry-Perot cavity, the light is sensitive to the normal displacement $u_z (z = 0, \mathbf{r}, t)$ of the coated plane face of the mirror, spatially averaged over the beam profile. This averaged displacement $\widehat{u}$ is defined as

$$\widehat{u}(t) = \int d^2r \; u_z (z = 0, \mathbf{r}, t) \frac{e^{-r^2/r_0^2}}{\pi r_0^2}. \qquad (10)$$

To compute the spectral density $S_{\widehat{u}} [\omega]$ of the displacement $\widehat{u}$ at a given angular frequency $\omega$, we determine the mechanical response of the mirror to a sinusoidally oscillating pressure. More precisely, we examine the effect of a pressure $P (\mathbf{r}, t)$ applied at every point $\mathbf{r}$ of the coated face of the mirror with the same spatial profile as the optical beam,

$$P (\mathbf{r}, t) = \frac{F_0}{\pi r_0^2} e^{-r^2/r_0^2} \cos (\omega t), \qquad (11)$$

where $F_0$ is a constant force amplitude. We can compute the energy $W_{diss}$ dissipated by the mirror in response to this force, averaged over a period $2\pi/\omega$ of the pressure oscillations. The fluctuation-dissipation theorem then states that the spectral density of the displacement noise is given by

$$S_{\widehat{u}} [\omega] = \frac{8 k_B T}{\omega^2} \frac{W_{diss}}{F_0^2}, \qquad (12)$$

where $k_B$ is the Boltzman's constant. This approach has been used by Levin to compute the brownian noise [18]. We are interested here in the thermodynamic noise so that $W_{diss}$ corresponds to the energy dissipated by thermoelastic heat flow.

The rate of thermoelastic dissipation is given by the following expression (first term of Eq. (35.1) of Ref. [19]):

$$W_{diss} = \left\langle T \frac{dS}{dt} \right\rangle = \left\langle \int d^3r \; \frac{\kappa}{T} (\nabla \delta T)^2 \right\rangle, \qquad (13)$$

where the integral is on the entire volume of the mirror and the brackets $\langle ... \rangle$ stand for an average over the oscillation period $2\pi/\omega$. $\delta T$ is the temperature perturbation around the unperturbed value $T$, induced by the oscillating pressure. $W_{diss}$ is then related to the time derivative $dS/dt$ of the mirror's entropy, which depends on the temperature gradient $\nabla \delta T$.

To calculate the rate of energy dissipation $W_{diss}$, it is necessary to solve a system of two coupled equations, the first one for the displacement $\mathbf{u} (\mathbf{r}, t)$ at every point $\mathbf{r}$ inside the substrate, and the second one for the temperature perturbation $\delta T (\mathbf{r}, t)$. As the time required for sound to travel across the mirror is usually smaller than the oscillation period $2\pi/\omega$, we can use a quasistatic approximation and deduce the displacement $\mathbf{u}$ from the equation of static stress balance [19],

$$\nabla (\nabla.\mathbf{u}) + (1 - 2\sigma) \nabla^2 \mathbf{u} = -2\alpha (1 + \sigma) \nabla \delta T, \qquad (14)$$

where $\sigma$ is the Poisson ratio of the substrate ($\alpha$ is the linear thermal expansion coefficient). The temperature perturbation $\delta T$ evolves according to the thermal conductivity equation [19],

$$\frac{\partial (\delta T)}{\partial t} - a^2 \Delta (\delta T) = \frac{-\alpha E T}{\rho C (1 - 2\sigma)} \frac{\partial (\nabla.\mathbf{u})}{\partial t}, \qquad (15)$$

where $a^2 = \kappa/\rho C$ and $E$ is the Young modulus of the substrate ($\rho$ is the density, $C$ is the specific thermal capacity).

The solutions of Eqs. (14) and (15) must also fulfill boundary conditions. If we approximate the mirror as a half space, the temperature perturbation $\delta T$ and the stress tensor $\sigma_{ij}$ must satisfy the following boundary conditions on the coated plane face of the mirror,

$$\sigma_{zz} (z = 0, \mathbf{r}, t) = P (\mathbf{r}, t), \qquad (16a)$$

$$\sigma_{zx} (z = 0, \mathbf{r}, t) = \sigma_{zy} (z = 0, \mathbf{r}, t) = 0, \qquad (16b)$$

$$\frac{\partial (\delta T)}{\partial z} (z = 0, \mathbf{r}, t) = 0. \qquad (16c)$$

The stress tensor $\sigma_{ij}$ is defined in presence of changes of temperature as (see Eq. (6.2) of [19])

$$\sigma_{ij} = -\frac{E}{(1 - 2\sigma)} \alpha \delta T \delta_{ij} +$$
$$+ \frac{E}{(1 + \sigma)} \left[ u_{ij} + \frac{\sigma}{(1 - 2\sigma)} \delta_{ij} \sum_k u_{kk} \right], \qquad (17)$$

where the strain tensor $u_{ij}$ is equal to $\frac{1}{2} \left( \frac{\partial u_i}{\partial x_j} + \frac{\partial u_j}{\partial x_i} \right)$.

We solve perturbatively this system of equations at the first order in $\alpha$. We first solve the static stress-balance equation at the zeroth order in $\alpha$, neglecting the temperature term in the right part of Eq. (14) and in the expression (17) of the stress tensor. The solution $\mathbf{u}^{(0)}$ of this equation is well known (paragraph 8 of [19]). We then solve the thermal conductivity equation (15) using as a source term the solution $\mathbf{u}^{(0)}$ and we obtain the temperature perturbation $\delta T^{(1)}$ in the first order in $\alpha$. The calculation of $\mathbf{u}^{(0)}$, $\delta T^{(1)}$ and finally $W_{diss}$ is done in Appendix A. Using the results of this appendix, we show that $S_{\widehat{u}} [\omega]$ is equal to

$$S_{\widehat{u}} [\omega] = 32 \alpha^2 (1 + \sigma)^2 \frac{k_B T^2}{\rho C} I, \qquad (18)$$

where the integral $I$ is given by

$$I = \frac{a^2}{(2\pi)^3} \int dk_x dk_y dk_z \frac{k_\perp^2 e^{-k_\perp^2 r_0^2/2}}{k^2 \left(a^4 k^4 + \omega^2\right)}, \qquad (19)$$

with $k_\perp^2 = k_x^2 + k_y^2$ and $k^2 = k_\perp^2 + k_z^2$.

We can express $S_{\widehat{u}}[\omega]$ as a function of an integral $J[\Omega]$ which depends only on a dimensionless variable $\Omega$ equal to $\omega/\omega_c$, where $\omega_c = a^2/r_0^2$ corresponds to the adiabatic limit (see Eq. 9). We get

$$S_{\widehat{u}}[\omega] = \frac{8}{\sqrt{2\pi}} \alpha^2 \left(1+\sigma\right)^2 \frac{k_B T^2 r_0}{\rho C a^2} J[\Omega], \qquad (20)$$

where $J[\Omega]$ is derived from the integral $I$ by the transformation of variables $u \equiv k_\perp r_0$ and $v \equiv k_z r_0$,

$$J[\Omega] = \sqrt{\frac{2}{\pi}} \int_0^\infty du \int_{-\infty}^\infty dv \frac{u^3 e^{-u^2/2}}{(u^2+v^2)\left((u^2+v^2)^2 + \Omega^2\right)}. \qquad (21)$$

When $\omega \gg \omega_c$ (i.e. $\Omega \gg 1$), we can neglect $u^2+v^2$ with respect to $\Omega$ in the denominator of the integral. $J[\Omega]$ can then be calculated analytically and we obtain

$$J[\Omega \gg 1] = 1/\Omega^2. \qquad (22)$$

Using this result and the definition of $\Omega$, we finally show that $S_{\widehat{u}}[\omega]$ is equal to

$$S_{\widehat{u}}[\omega \gg \omega_c] = \frac{8}{\sqrt{2\pi}} \alpha^2 \left(1+\sigma\right)^2 \frac{k_B T^2}{\rho C} \frac{a^2}{\omega^2 r_0^3}. \qquad (23)$$

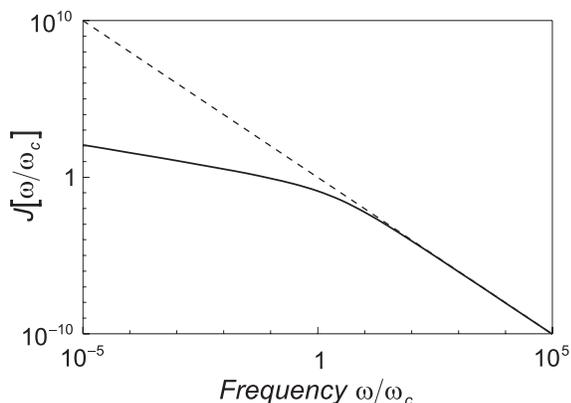This formula is identical to the expression (18) of Ref. [3] and to the expression (12) of BGV [1].



FIG. 1. Frequency dependence of the thermodynamic noise. The frequency $\omega$ is normalized to the adiabatic limit $\omega_c$. The dashed curve corresponds to the adiabatic approximation.

For small values of $\Omega$, the integral $J[\Omega]$ can be computed numerically. The result is shown in figure 1 where we have plotted $J[\Omega]$ as a function of $\Omega$ in logarithmic

scale, for $\Omega$ between $10^{-5}$ and $10^5$. This figure shows that $\Omega = 1$ is a cut-off frequency. For $\Omega > 1$ the curve has a slope equal to $-2$, whereas for $\Omega < 1$ the curve has a smaller slope of the order of $-1/2$. In this low frequency range, the noise is smaller than the one which would be obtained using the adiabatic approximation (dashed curve in figure 1).

## IV. PHOTOTHERMAL NOISE

We now briefly examine the case of the photothermal noise which exhibits somewhat a similar frequency behaviour as the thermodynamic noise. We use the same method as BGV [1] to calculate the spectral density $S_{\widehat{u}}[\omega]$ due to this noise but we do not make any adiabatic approximation so that the calculation is valid also for frequencies smaller than the adiabatic limit $\omega_c$. We then obtain:

$$S_{\widehat{u}}[\omega] = \frac{2}{\pi^2} \alpha^2 \left(1+\sigma\right)^2 \frac{\hbar \omega_0 W_{abs}}{\left(\rho C a^2\right)^2} K[\Omega], \qquad (24)$$

where the integral $K[\Omega]$ is equal to

$$K[\Omega] = \left| \frac{1}{\pi} \int_0^\infty du \int_{-\infty}^\infty dv \frac{u^2 e^{-u^2/2}}{(u^2+v^2)(u^2+v^2+i\Omega)} \right|^2. \qquad (25)$$

When $\omega \gg \omega_c$ the adiabatic approximation is valid and the result of BGV should be recovered. Indeed, when $\Omega \gg 1$, we can neglect $u^2 + v^2$ with respect to $\Omega$ and calculate analytically $K[\Omega]$ which turns out to be equal to $1/\Omega^2$. Using the definition of $\Omega$, we finally show that $S_{\widehat{u}}[\omega]$ is equal to

$$S_{\widehat{u}}[\omega \gg \omega_c] = \frac{2}{\pi^2} \alpha^2 \left(1+\sigma\right)^2 \frac{\hbar \omega_0 W_{abs}}{\left(\rho C r_0^2 \omega\right)^2}. \qquad (26)$$

This formula is identical to Eq. (8) of BGV [1].

For low values of $\Omega$, $K[\Omega]$ can be calculated numerically. The result is shown in figure 2. As in the case of the thermodynamic effect (figure 1), $\Omega = 1$ is a cut-off frequency: for $\Omega > 1$ the function has a slope equal to $-2$, whereas for $\Omega < 1$ the function has a much smaller slope and is almost constant.

This result is in perfect agreement with the simple derivation made in section II. The spectral density (24) can actually be written as

$$S_{\widehat{u}}[\omega] = \frac{2}{\pi^2} \left(1+\sigma\right)^2 \left(\frac{\alpha}{\kappa}\right)^2 S_{abs} K[\Omega], \qquad (27)$$

which is similar to Eq. (8) at low frequency where $K[\Omega] \simeq 1$, apart from a term with the Poisson ratio. The frequency dependence of the photothermal noise then corresponds to a low-pass filter, with a cut-off frequency equal to the adiabatic limit $\omega_c$. At low frequency, that
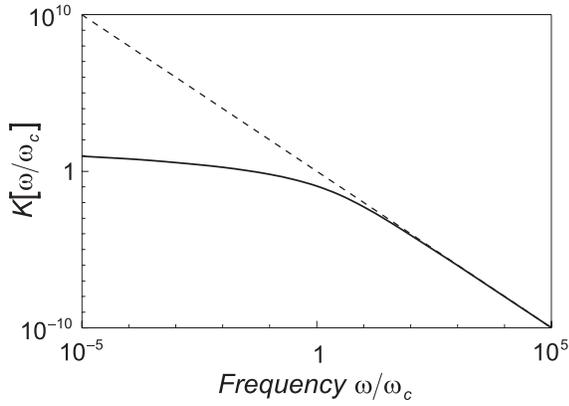
FIG. 2. Frequency dependence of the photothermal noise. The frequency $\omega$ is normalized to the adiabatic limit $\omega_c$. The dashed curve corresponds to the adiabatic approximation.

is when the thermal diffusion length $l_t$ in the substrate becomes larger than the beam spot radius $r_0$, one has a dramatic change of regime and the photothermal noise is much smaller than the one which would be obtained within the adiabatic approximation (dashed curve in figure 2).

Another important point for the realization of optomechanical sensors working at the quantum level is to compare the photothermal noise to the displacements induced by the quantum fluctuations of radiation pressure of light. Quantum effects can be made larger than the usual thermal noise by decreasing the temperature and by increasing the light power. This would not be convenient for photothermal noise since the effect is proportional to the light power. BGV results show that for sapphire at room temperature the photothermal noise is of the same order as the standard quantum limit in an interferometer. In a high-finesse cavity, hopefully, these two effects are related to quite different photon statistics. As a matter of fact, the displacement $\widehat{u}$ induced by the radiation pressure of the intracavity field is related to the intracavity photon flux $N$,

$$\widehat{u}[\omega] = \chi_{eff}[\omega] P_{rad}[\omega] = 2\hbar k \chi_{eff}[\omega] N[\omega], \quad (28)$$

where $2\hbar k$ is the momentum exchange during a photon reflection ($k$ is the wavevector of light), and $\chi_{eff}$ is an effective susceptibility describing the mechanical response of the mirror to the radiation pressure $P_{rad}$ [12]. The noise spectrum $S_{\widehat{u}}[\omega]$ induced by radiation pressure is thus proportional to the spectral power noise $S_{cav}$ of the intracavity light, which for a resonant cavity is [12]:

$$S_{cav}[\omega] = \frac{2\mathcal{F}/\pi}{1 + (\omega/\omega_{cav})^2} \hbar \omega_0 W_{cav}, \quad (29)$$

where $\omega_{cav}$ is the cavity bandwidth, $\mathcal{F}$ is the cavity finesse and $W_{cav} = \hbar \omega_0 \overline{N}$ is the average intracavity light power. At low frequency ($\omega \lesssim \omega_{cav}$) the intracavity photon flux corresponds to a super-poissonian statistics,

the noise power being larger than the poissonian spectral density by a factor $2\mathcal{F}/\pi$ [20].

On the other hand, the absorbed photons always corresponds to a poissonian statistics, even if it is not the case for the intracavity photons. The spectral power noise $S_{abs}$ of the absorbed light is given by

$$S_{abs} = \hbar \omega_0 W_{abs} = A \hbar \omega_0 W_{cav}, \quad (30)$$

where $A$ is the absorption coefficient of the mirror (the average flux of absorbed photons is $\overline{n} = A\overline{N}$). This effect cannot be understood within the framework of a corpuscular model in which the photon absorption is described as a poissonian process: due to the super-poissonian statistics of the intracavity photons, one would find a super-poissonian statistics for the absorbed photons. One has to take into account the interferences between the intracavity field and the vacuum fluctuations associated with the mirror losses. This can be done by using a simple model where the absorption is described as a small transmission of the mirror and where the absorbed photons are identified to the photons transmitted by the mirror. One thus has a high-finesse cavity with two input-output ports and it is well known that the photon statistics of the light either reflected or transmitted by such a cavity are always poissonian, for coherent or vacuum incoming beams [21].

Eqs. (29) and (30) clearly show that both the radiation pressure effect and the photothermal noise are proportional to the intracavity light power $W_{cav}$; however the displacements induced by radiation pressure have an extra dependence on the cavity finesse $\mathcal{F}$. The photothermal noise can thus become negligible as compared to quantum effects for a high-finesse cavity.

To perform a quantitative comparison between the two effects, we calculate the susceptibility $\chi_{eff}$ defined by Eq. (28). We determine here the mechanical response associated with the internal degrees of freedom of the mirror, which are of interest for displacement sensors. We thus ignore the radiation pressure effects associated with the global motion of suspended mirrors, which are the dominant contribution to SQL at low frequency in gravitational-wave interferometers. We calculate the average displacement $\widehat{u}$ induced by the radiation pressure $P_{rad}$, assuming the mirror is a half space ($z \geq 0$). The normal displacement $u_z(z = 0, \mathbf{r}, t)$ of the coated face of the mirror can be deduced from the results of paragraph 8 of [19],

$$u_z(z = 0, \mathbf{r}, t) = \frac{2\hbar k N(t)}{E\pi^2 r_0^2} (1 - \sigma^2) \int d^2 r' \frac{e^{-r'^2/r_0^2}}{|\mathbf{r} - \mathbf{r}'|}. \quad (31)$$

Using the definition (10) of $\widehat{u}$, we obtain

$$\widehat{u}(t) = \frac{2\hbar k N(t)}{E\pi^3 r_0^4} (1 - \sigma^2) \int d^2 r d^2 r' \frac{e^{-(r^2 + r'^2)/r_0^2}}{|\mathbf{r} - \mathbf{r}'|}. \quad (32)$$

The integral can easily be calculated by using a new set of variables $\mathbf{u} = \mathbf{r} - \mathbf{r}'$ and $\mathbf{v} = \mathbf{r} + \mathbf{r}'$. We finally get

$$\chi_{eff}[\omega] = \frac{1 - \sigma^2}{\sqrt{2\pi} E r_0}, \tag{33}$$

and the noise spectrum $S_{\widehat{u}}[\omega]$ induced by radiation pressure fluctuations is equal to

$$S_{\widehat{u}}[\omega] = \left(\frac{2\left(1 - \sigma^2\right)}{\sqrt{2\pi} E c r_0}\right)^2 S_{cav}[\omega], \tag{34}$$

where $c$ is the speed of light.

For all the displacement sensors considered in this paper the characteristic angular frequency $\omega$ is smaller than the cavity bandwidth $\omega_{cav}$. The noise spectrum $S_{\widehat{u}}[\omega]$ is consequently independent of $\omega$ and equal to

$$S_{\widehat{u}}[\omega \ll \omega_{cav}] = \left(\frac{2\left(1 - \sigma^2\right)}{\sqrt{2\pi} E c r_0}\right)^2 \frac{2\mathcal{F}}{\pi} \hbar \omega_0 W_{cav}. \tag{35}$$

This expression shows that the radiation pressure effect depends on the mechanical characteristics of the substrate ($E$ and $\sigma$) whereas the photothermal noise (Eq. 27) depends on the thermodynamic characteristics of the substrate via the ratio $\alpha/\kappa$. At low temperature, $K[\Omega]$ is of the order of 1 and the ratio $\alpha/\kappa$ is constant and equal to $1.4\ 10^{-13}\ m/W$ for sapphire (see Table I). $E$ is equal to $4\ 10^{11}\ J/m^3$ and $\sigma$ is equal to 0.25 so that the ratio between the photothermal and radiation pressure noises is of the order of

$$S_{\widehat{u}}^{pt}/S_{\widehat{u}}^{rad} \simeq 2.5\ 10^{14} \frac{A r_0^2}{\mathcal{F}}. \tag{36}$$

For a 1 $ppm$ absorption rate ($A = 10^{-6}$), a beam spot size $r_0$ of $10^{-4}\ m$, and a cavity finesse $\mathcal{F}$ of $10^5$, the photothermal noise is more than 4 orders of magnitude smaller than the radiation pressure effects of internal degrees of freedom of the mirror. The photothermal noise is thus negligible as compared to quantum effects in optomechanical sensors.

Note that this is not the case in gravitational-wave interferometers where $r_0 \simeq 10^{-2}\ m$ and $\mathcal{F} \simeq 100$. The photothermal noise is then 2 orders of magnitude larger than the quantum noise of internal motion. However, the interferometer is not expected to be sensitive to this quantum noise since for suspended mirrors it is overwhelmed by the quantum noise associated with external pendulum motion.

## V. DISCUSSION AND CONCLUSION

We have shown that both thermoelastic and photothermal noises have a frequency dependence which looks like a low-pass filter: below a cut-off frequency $\omega_c$, these noises are much smaller than the noise which would be obtained according to the $1/\omega^2$ dependence at high-frequency.

First lines in tables II give the values of the cut-off frequency $\omega_c/2\pi$ for fused silica and sapphire, and for a beam spot size $r_0$ of 1 $cm$ (first table) and $10^{-2}\ cm$ (second table). The results show that $\omega_c$ is increased when the temperature decreases (3 orders of magnitude for fused silica and 6 orders of magnitude for sapphire when the temperature is reduced from 300 $K$ to 1 $K$). If we consider a typical frequency $\omega/2\pi$ of 100 $Hz$, the adiabatic approximation is never valid for sapphire at low temperature, whereas it is valid for fused silica only for large beam spot size.

| $r_0 = 10^{-2}\ m$ | Fused silica | | Sapphire | |
|---|---|---|---|---|
| | 300 $K$ | 1 $K$ | 300 $K$ | 1 $K$ |
| $\omega_c/2\pi$ ($Hz$) | $1.5\ 10^{-3}$ | 4.8 | $2\ 10^{-2}$ | $1.9\ 10^4$ |
| $\Omega^2 J[\Omega]$ | 1 | 0.74 | 0.98 | $1.3\ 10^{-4}$ |
| $S_{\widehat{u}}$ ($m^2/Hz$) | $2.7\ 10^{-42}$ | $3.4\ 10^{-45}$ | $1.5\ 10^{-39}$ | $2.6\ 10^{-49}$ |
| $S_{\widehat{u}}$ (adiabatic) | $2.7\ 10^{-42}$ | $4.6\ 10^{-45}$ | $1.5\ 10^{-39}$ | $2\ 10^{-45}$ |

| $r_0 = 10^{-4}\ m$ | Fused silica | | Sapphire | |
|---|---|---|---|---|
| | 300 $K$ | 1 $K$ | 300 $K$ | 1 $K$ |
| $\omega_c/2\pi$ ($Hz$) | 15 | $4.8\ 10^4$ | $2\ 10^2$ | $1.9\ 10^8$ |
| $\Omega^2 J[\Omega]$ | 0.51 | $3.5\ 10^{-5}$ | $6.4\ 10^{-2}$ | $1.4\ 10^{-10}$ |
| $S_{\widehat{u}}$ ($m^2/Hz$) | $1.4\ 10^{-36}$ | $1.6\ 10^{-43}$ | $1\ 10^{-34}$ | $2.8\ 10^{-49}$ |
| $S_{\widehat{u}}$ (adiabatic) | $2.7\ 10^{-36}$ | $4.6\ 10^{-39}$ | $1.6\ 10^{-33}$ | $2\ 10^{-39}$ |

TABLE II. Results for fused silica and sapphire at different temperatures, for a frequency $\omega/2\pi = 100\ Hz$ and for a beam spot size $r_0 = 1\ cm$ (top) and $10^{-2}\ cm$ (bottom). The thermodynamic noise $S_{\widehat{u}}$ ($3^{rd}$ lines) is reduced as compared to its value obtained within the adiabatic approximation ($4^{th}$ lines) by a factor $\Omega^2 J[\Omega]$ ($2^{nd}$ lines).

We first focus on the thermodynamic noise whose values calculated from Eq. (20) are shown in the third lines of tables II. The noise is smaller than the one which would be obtained within the adiabatic approximation (last lines in tables II). The reduction factor, equal to $1/\Omega^2 J[\Omega]$, can be as large as $10^4$ for sapphire at low temperature with $r_0 = 1\ cm$, and as large as $10^{10}$ for $r_0 = 10^{-2}\ cm$ (second lines in tables II).

We immediately see the impact for gravitational-wave interferometers ($r_0 = 1\ cm$): for sapphire at low temperature, the thermodynamic noise is more than 4 order of magnitude smaller than for fused silica, so that the choice of the material at low temperature would be just the opposite than, as in BGV, at room temperature. Furthermore, the thermodynamic noise at 100 $Hz$ would be equal to $2.6\ 10^{-49}\ m^2/Hz$ for sapphire at low temperature, well below the noise at room temperature ($2.7\ 10^{-42}\ m^2/Hz$ for fused silica). It is also well below the SQL limit due to the external pendulum motion, equal to $3.6\ 10^{-41}\ m^2/Hz$ for a mirror mass of 30 $kg$ [1].

Similarly for optomechanical systems with smaller beam spot size ($r_0 \lesssim 10^{-2}\ cm$), the thermodynamic

noise can be made as small as $2.8 \ 10^{-49} \ m^2/Hz$ by using sapphire at low temperature, to be compared to a noise larger than $10^{-36} \ m^2/Hz$ at room temperature both for sapphire and fused silica. It is worth noticing that this very low value is partly due to the reduction factor associated with the non adiabaticity which is of the order of $10^{10}$. This noise can be compared to the SQL limit due to the internal motion of the mirror, which is equal to $\hbar |\chi_{eff}| \simeq 10^{-42} \ m^2/Hz$ [22]. At low temperature, the thermodynamic noise is thus smaller than the SQL limit so that optomechanical sensors as in Refs. [9,10] would be able to get to the SQL limit.

Let us note that the thermodynamic noise for sapphire at $1 \ K$ is mostly independent of the beam spot size $r_0$: similar values are obtained for large spot sizes ($2.6 \ 10^{-49} \ m^2/Hz$ for $r_0 = 1 \ cm$) and small ones ($2.8 \ 10^{-49} \ m^2/Hz$ for $r_0 = 10^{-2} \ cm$). This result is due to the fact that, in contrast with fused silica, the adiabatic approximation is not valid for sapphire whatever the beam spot size is, as long as it is smaller than a few centimeters. The non adiabatic condition $\omega < \omega_c$ can actually be written as $r_0 < \sqrt{\kappa/\rho C \omega}$ (see Eq. 9). In this non adiabatic regime, we have shown that $J[\Omega]$ evolves as $1/\sqrt{\Omega}$ which is proportional to $\sqrt{\omega_c}$ and then to $1/r_0$. The thermodynamic noise is proportional to $r_0 J[\Omega]$ (Eq. 20) and is then independent of $r_0$.

Similar results can be obtained for the photothermal noise. We have shown that as long as the adiabatic condition is not satisfied, the noise mostly depends on the ratio $\alpha/\kappa$ (Eqs. 8 or 27). In particular it does not depend on the frequency $\omega$ nor on the beam spot size $r_0$. For sapphire at low temperature and for an average absorbed power $W_{abs} \simeq 1 \ W$ of Nd-Yag laser light, the photothermal noise is then of the order of $10^{-45} \ m^2/Hz$ both for interferometers and optomechanical sensors, well below the SQL limits of both the external and internal motions.

Let us finally note that the results obtained above apply in detail to an actual mirror system when the conditions described in section II are fulfilled. In particular the interplay of the various characteristic lengths (phonon mean free path and thermal lengths at the frequencies of interest, both in the substrate and in the coating, beam spot, coating thickness and mirror size) must in the end allow, in some temperature range, that the thermal properties of the substrate dominate.

This may be not easy to achieve and thus our analysis may correspond to a somewhat idealized situation. At the lowest temperatures $T \leq 0.5 \ K$, the phonon mean free path in the coating gets of the order of its thickness (as for an amorphous silica coating, see for example [16]), while the time constants for phonon local equilibrium continue to stay smaller than $2\pi/\omega$ both for the coating and the substrate. At first sight, it may appear that the equalization of coating versus substrate temperatures will be even more facilitated. However at some intermediate temperature below $10 \ K$ the phonon mean

free path in substrates like sapphire may get so long to exceed the dimensions of the mirror. In this case a more ad hoc model has to be considered, in which one specifies the details of the thermal link of the mirror to the main heat sink. Similar care should be taken if the thermal length at the lowest frequency of interest is of the order of the mirror size. Possibly in both cases the effect would be smaller than predicted in this paper, because the characteristic times for thermal equilibrium in the mirror volume would get even shorter. In any case, as to quote just one instance, phonon mean free paths and thermal conductivities (and thus thermal lengths), have strong dependencies at low temperatures on the level of impurities, so that each experimental configuration may be a case per se.

In conclusion our results may be possibly of interest in two respects. First because they let see promising the use of low temperatures both for gravitational-wave interferometers and for optomechanical devices. Second because they may be of help to study, in actual experimental configurations for SQL conditions, the role of the thermoelastic effects in respect to choices of substrate materials, working temperatures, cavity finesses, mirrors losses, beam spot sizes and laser powers.

## APPENDIX A

In this appendix, we calculate the spectral density $S_{\widehat{u}}[\omega]$ (Eq. 18) of the spatially averaged displacement $\widehat{u}$ induced by the thermodynamic noise. We approximate the mirror as an infinite half space ($z \geq 0$). At the zeroth order in the thermal expansion coefficient $\alpha$, the solution $\mathbf{u}^{(0)}$ of the quasistatic stress balance equation (14) is given by a Green's tensor (Eqs. (8.13) and (8.18) of [19]). The pressure $P(\mathbf{r}, t)$ applied on the coated surface of the mirror has only a component along the normal axis $z$, and we obtain the following expression for the displacement expansion $\Theta^{(0)} = \nabla.\mathbf{u}^{(0)}$,

$$\Theta^{(0)}(\mathbf{r}, t) = -\frac{2(1+\sigma)(1-2\sigma)}{E} F_0 \cos(\omega t) \times$$
$$\times \int \frac{dk_x dk_y}{(2\pi)^2} e^{-\frac{1}{4} k_\perp^2 r_0^2 - k_\perp z + i(k_x x + k_y y)}, \quad (37)$$

with $k_\perp = \sqrt{k_x^2 + k_y^2}$.

To calculate the dissipated energy $W_{diss}$ it is useful to analytically extend the pressure-induced expansion $\Theta^{(0)}$ for negative values of $z$ in such a way that it is an even function of $z$. Its spatial Fourier transform $\Theta^{(0)}[\mathbf{k}, t]$ is then equal to

$$\Theta^{(0)}[\mathbf{k}, t] = -\frac{4(1+\sigma)(1-2\sigma)}{E} F_0 \cos(\omega t) \frac{k_\perp}{k^2} e^{-\frac{1}{4} k_\perp^2 r_0^2}, \quad (38)$$

with $k^2 = k_x^2 + k_y^2 + k_z^2$.

In the same way, we analytically extend the temperature perturbation $\delta T$ in the half space $z \leq 0$ in such a way that $\delta T^{(1)}(\mathbf{r}, t)$ is an even function of $z$. Using the Fourier transform of the thermal conductivity equation (15) and the expression (38) of $\Theta^{(0)}$, we find that $\delta T^{(1)}[\mathbf{k}, t]$ is equal to

$$\delta T^{(1)}[\mathbf{k}, t] = A[\mathbf{k}] e^{i\omega t} + c.c., \quad (39)$$

where the function $A[\mathbf{k}]$ is given by

$$A[\mathbf{k}] = \frac{2(1+\sigma)\alpha T}{\rho C} \frac{i\omega k_\perp}{k^2(a^2 k^2 + i\omega)} F_0 e^{-\frac{1}{4} k_\perp^2 r_0^2}. \quad (40)$$

We now determine the thermoelastic dissipation $W_{diss}$. The integral over $z$ in Eq. (13) is limited to the volume of the mirror (infinite half space $z \geq 0$). Since $\delta T^{(1)}(\mathbf{r}, t)$ is an even function of $z$, $W_{diss}$ can be written as

$$W_{diss} = \frac{\kappa}{2T} \left\langle \int d^3 r \left( \nabla \delta T^{(1)} \right)^2 \right\rangle, \quad (41)$$

where the spatial integration is in the whole space. Using the Bessel-Perseval relation, we can express the dissipated energy $W_{diss}$ as a function of the temporal average of $\left| \delta T^{(1)}[\mathbf{k}, t] \right|^2$ which is equal to $2 |A[\mathbf{k}]|^2$ (Eq. 39):

$$W_{diss} = \frac{\kappa}{2T} \int \frac{d^3 k}{(2\pi)^3} k^2 \left\langle \left| \delta T^{(1)}[\mathbf{k}, t] \right|^2 \right\rangle$$
$$= \frac{\kappa}{T} \int \frac{d^3 k}{(2\pi)^3} k^2 |A[\mathbf{k}]|^2. \quad (42)$$

Using Eq. (40), we finally obtain

$$\frac{W_{diss}}{F_0^2} = \frac{4T}{\rho C} \alpha^2 (1+\sigma)^2 \omega^2 I, \quad (43)$$

where the integral $I$ is given by

$$I = \int \frac{d^3 k}{(2\pi)^3} \frac{a^2 k_\perp^2}{k^2 (a^4 k^4 + \omega^2)} e^{-k_\perp^2 r_0^2 / 2}. \quad (44)$$

This expression allows to determine the spectral density $S_{\widehat{u}}[\omega]$ of the displacement $\widehat{u}$ from the fluctuation-dissipation theorem (Eq. 12). One gets the result given in the text by Eq. (18):

$$S_{\widehat{u}}[\omega] = 32\alpha^2 (1+\sigma)^2 \frac{k_B T^2}{\rho C} I. \quad (45)$$

[1] V.B. Braginsky, M.L. Gorodetsky and S.P. Vyatchanin, *Phys. Lett. A* **264**, 1 (1999)
[2] See for instance P.R. Saulson, *Phys. Rev. D* **42**, 2437 (1990)
[3] Y.T. Liu and K.S. Thorne, *Phys. Rev. D*, in press (2000)
[4] E. Gustafson *et al*, LSC white paper on detector research and development, LIGO T990080-00-D (1999)
[5] C.M. Caves, *Phys. Rev. D* **23**, 1693 (1981)
[6] V.B. Braginsky and F.Ya. Khalili, *Quantum measurement*, edited by K.S. Thorne (Cambridge University Press, 1992)
[7] K. Kuroda *et al*, *Int. Journ. Mod. Phys. D* **8**, 537 (1999)
[8] A. Giazotto, private communication
[9] L. Conti *et al*, *Rev. Sci. Instrum.* **69**, 554 (1998)
[10] P.F. Cohadon, A. Heidmann and M. Pinard, *Phys. Rev. Lett.* **83**, 3174 (1999)
[11] M. Pinard, Y. Hadjar and A. Heidmann, *Eur. Phys. J. D* **7**, 107 (1999)
[12] A. Heidmann, Y. Hadjar and M. Pinard, *Appl. Phys. B* **64**, 173 (1997)
[13] R. Berman, E.L. Foster and J.M. Ziman, *Proc. Roy. Soc. A* **231**, 130 (1955)
[14] R.C. Zeller and R.O. Pohl, *Phys. Rev. B* **4**, 2029 (1971)
[15] R. Liu, S. Schiller and R.L. Byers, Stanford University, internal report (1993) and references therein
[16] P.D. Vu, Xiao Liu and R.O. Pohl, arXiv:cond-mat/0002413
[17] W.A. Little, *Can. Journ. Phys.* **37**, 334 (1959)
[18] Yu. Levin, *Phys. Rev. D* **57**, 659 (1998)
[19] L.D. Landau and E.M. Lifshitz, *Theory of Elasticity*, third edition (Pergamon, Oxford, 1986)
[20] M.C. Teich and B.E.A. Saleh, in *Progress in Optics XXVI*, edited by E. Wolf (North-Holland, Amsterdam, 1988)
[21] S. Reynaud, A. Heidmann, E. Giacobino and C. Fabre, in *Progress in Optics XXX*, edited by E. Wolf (North-Holland, Amsterdam, 1992)
[22] M.T. Jaekel and S. Reynaud, *Europhys. Lett.* **13**, 301 (1990)
[23] V.B. Braginsky and S.P. Vyatchanin, private communication
[24] S. Rowan, M.M. Fejer, E. Gustavson, R. Route, J. Hough, G. Cagnoli and P. Sneddon, Aspen 2000 Winter Conference on Gravitational Waves and their Detection (unpublished)